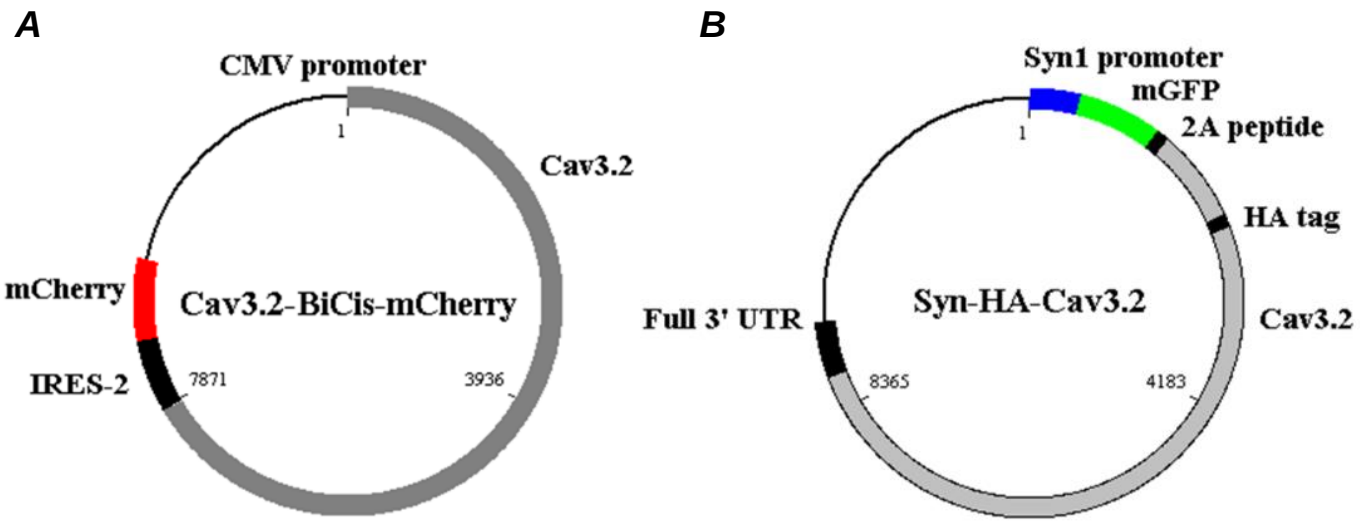

Supplementary figure 1: Maps of the plasmids engineered for this study. *A*, map of the plasmid used for the electrophysiology recordings. The plasmid contains a CMV promoter driving the channel cDNA and mCherry separated by IRES-2 (Clontech). *B*, map of the plasmid used for the trafficking experiments. This plasmid used a fragment of the human synapsin-1 promoter to drive expression of GFP and the channel separated by a a 2A peptide bridge.

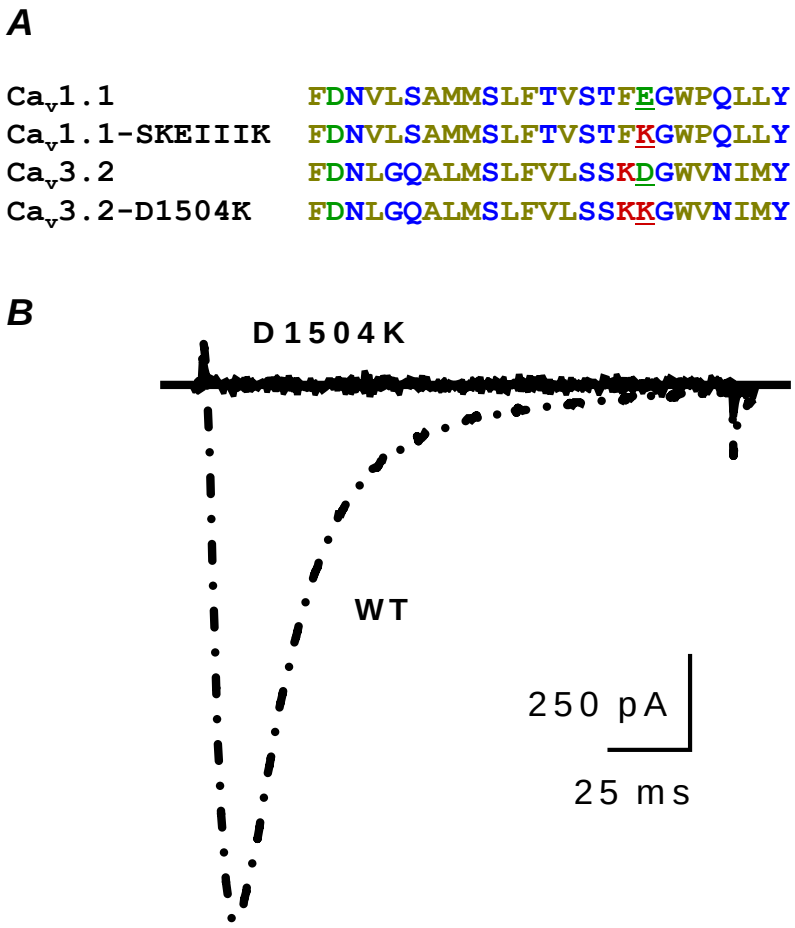

Supplemental figure 2: Characterization of the non-coducting mutant. *A*, alignment of the human $Ca_v1.1$ and $Ca_v3.2$ channels and the respective mutants SKEIIIK (Dirksen *et al.*, 1999) and D1504K. Underlining highlights the amino acids that are altered in the mutated channels. *B*, representative current traces from transfected HEK-293 cells showing the absence of currents in the D1504K mutant.

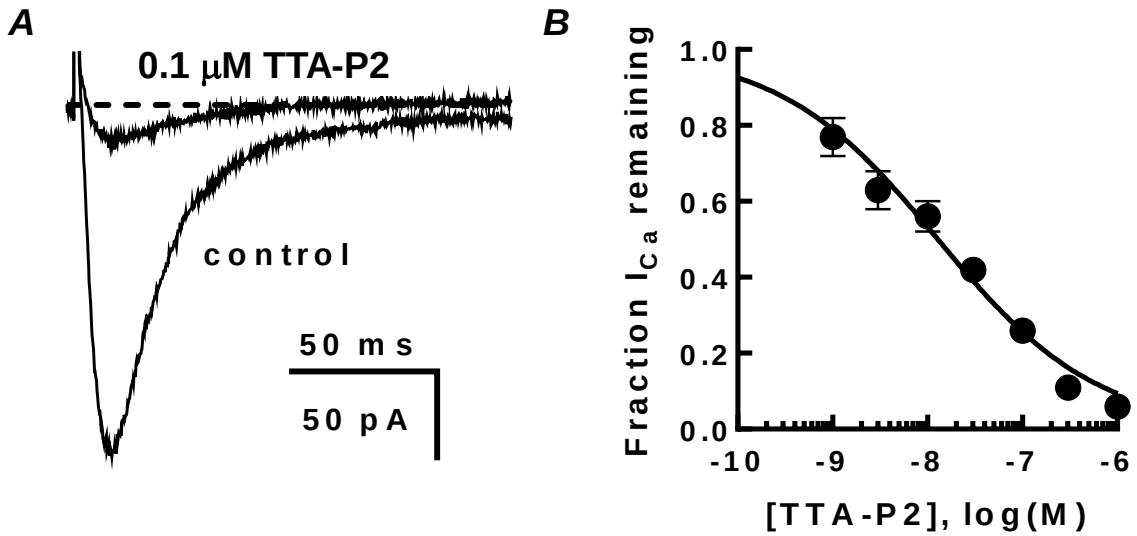

Supplemental figure 3: Potency of TTA-P2 at blocking recombinant $Ca_v3.2$ currents in HEK-293 cells. *A*, representative traces showing the effect of the selective T-type channel blocker TTA-P2 for control and after wash-in of 0.1 μM TTA-P2. *B*, TTA-P2 efficiently blocked T-type current in HEK-293 cells expressing recombinant $Ca_v3.2$ channels. The apparent IC_{50} was 13 nM.

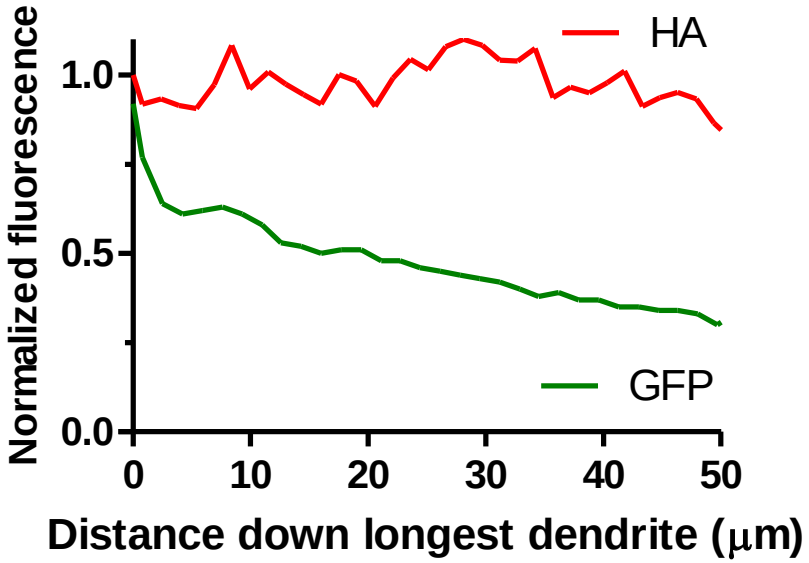

Supplementary figure 4: Trafficking of GFP and the T-channel into the main dendrite differ. The peak of the GFP signal was found at the cell body and decayed down the length of the dendrite. In contrast, HA-tagged channels labeled with a red fluorophore displayed a non-decaying signal along the dendrite. This provides evidence the two proteins were expressed independently.

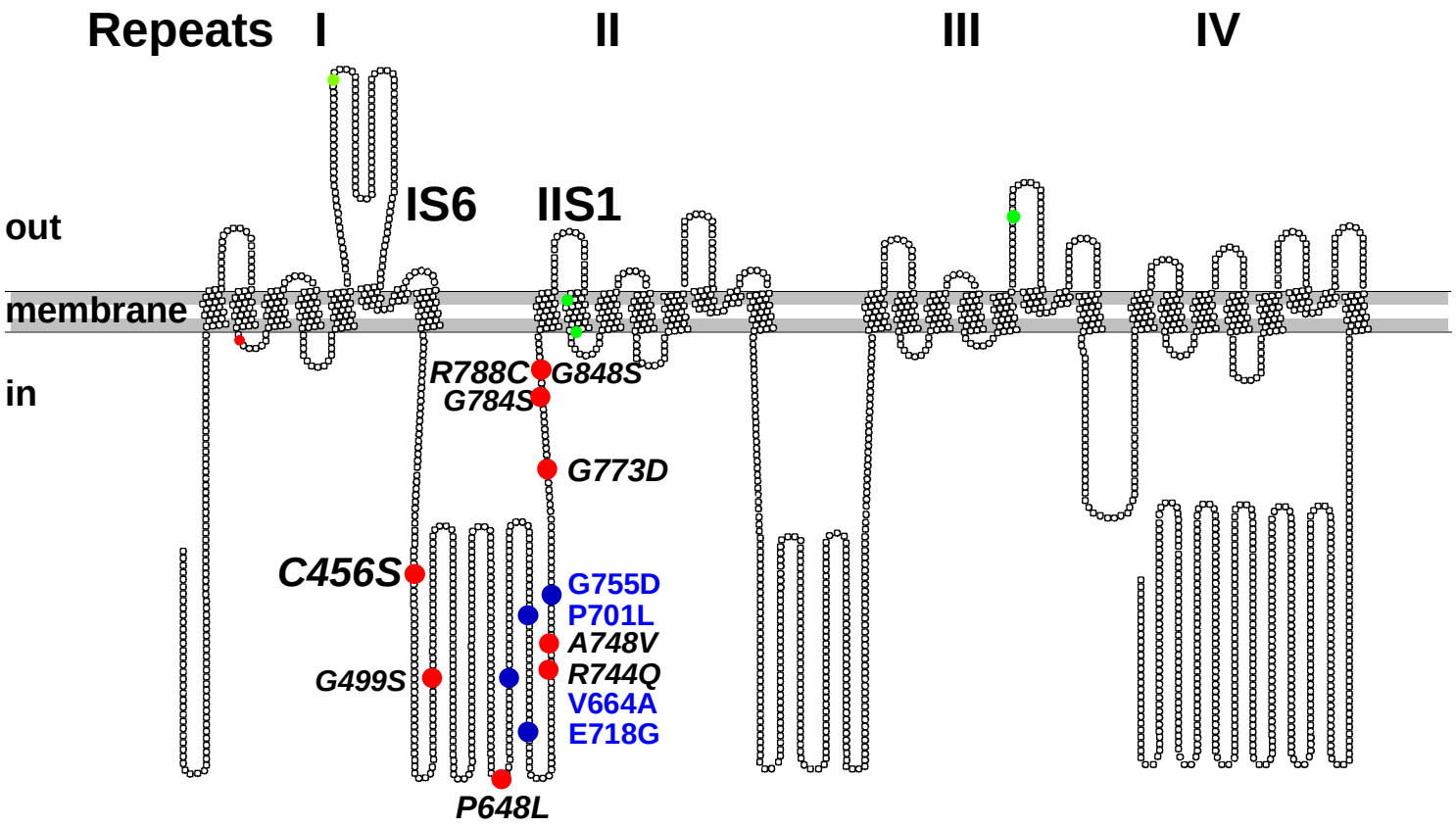

Supplemental figure 5. Location of the CAE variants. The $Ca_V3.2$ channel is illustrated with every amino acid represented with a circle. The *location of the mutations found in the I-II intracellular loop are highlighted as follows:* mutations found in Chinese CAE patients are shown in black (Chen *et al*., 2003); while mutations found only in idiopathic epilepsy patients in the Baylor Ion Channel Project are shown in blue (Klassen *et al*., 2011). The deletion mutants removed the following amino acids: D1, 429-452; D2, 453-491; D3, 493-539; D4, 540-618; and D5, 619-772 (Vitko *et al*., 2007). The amino acids mutated in the AARA mutant are Y479A, R481A, and W482A.

Supplemental figure 6: The AARA variant expressed in HEK-293 cells had little or no effect on channel biophysics. *A*, Average IV relationships normalised to cell capacitance using during depolarising voltage steps from -80 to -10 mV (holding potential -100 mV) in WT and AARA. (n= 23, WT; 19, AARA). Error bars are omitted for clarity. *B*, IV data were normalised to the maximum inward current in each cell and then averaged. *C*, the normalised amplitude obtained during a 20 ms test pulse to -20 mV preceded by incremental hyperpolarising pulses (15 s) from -80 mV. *D*, the conductance normalised to current density was slightly reduced in AARA compared to WT. *E*, activation time did not differ between WT and AARA. *F*, the inactivation time was slower in AARA compared to WT condition Statistical significance at P<0.05 with a single asterisk and at P<0.001 with a triple asterisk, Student's t-test.